List of Figures

List of Tables

NOTES

I have collected all of the data figures from chapter 4 of my thesis. Please help me check the language, grammar, and accuracy of the captions! I would also appreciate suggestions on how to make the figures communicate the main points more clearly.

Some lingering issues:

Do people prefer the $\nu_2' + 2\nu_3'$ notation or the $2^1 3^2$ notation? I think the former is easier to understand for non-spectroscopists, but it is definitely the uglier of the two.

Can I get rid of some of the repeated phrases in the captions, without changing the order of the figures?

Do I need to include legends in the figures of c.o.g. vs. time? The upper state quantum number is labeled to the right, but the legend may help readers follow the lines as they cross in the plot.

Thank you, early readers!

Table 4.1: Term values of the acetylene $\tilde{A}\,{}^1A_u$ vibrational levels considered in this study. The energies of all four levels are in the critical region above the $S_1 \sim T_3$ electronic seam of intersection ($\simeq 45300$ cm^{-1}) but below the first dissociation barrier ($\simeq 46300$ cm^{-1}).

Level		Term value (cm^{-1})
$2\nu_2' + \nu_3'$	K_a=1	46010
$2\nu_3' + 2\nu_4'$	K_a=1	45812
$\nu_2' + 2\nu_3'$	K_a=1	45677
$3\nu_3'$	K_a=2	45352

Figure 4-1: Simultaneously recorded SEELEM (upper trace) and LIF (lower trace) spectra of the $\nu_2'+2\nu_3'$ K_a=1 sublevel of the $\tilde{A}^1A_u \leftarrow \tilde{X}^1\Sigma_g^+$ electronic transition. The LIF spectrum is integrated in two time regions: an early time window ($0.5\tau_s - 2\tau_s$, solid trace) and a delayed time window ($10\tau_s - 18\tau_s$, dashed trace). The Q(1) and Q(2) transitions are redshifted in the delayed fluorescence spectrum, in contrast to the Q(3,4,5) transitions. The P(2) transition, having the same J' but opposite parity from Q(1), shows a similar redshift in the delayed fluorescence spectrum.

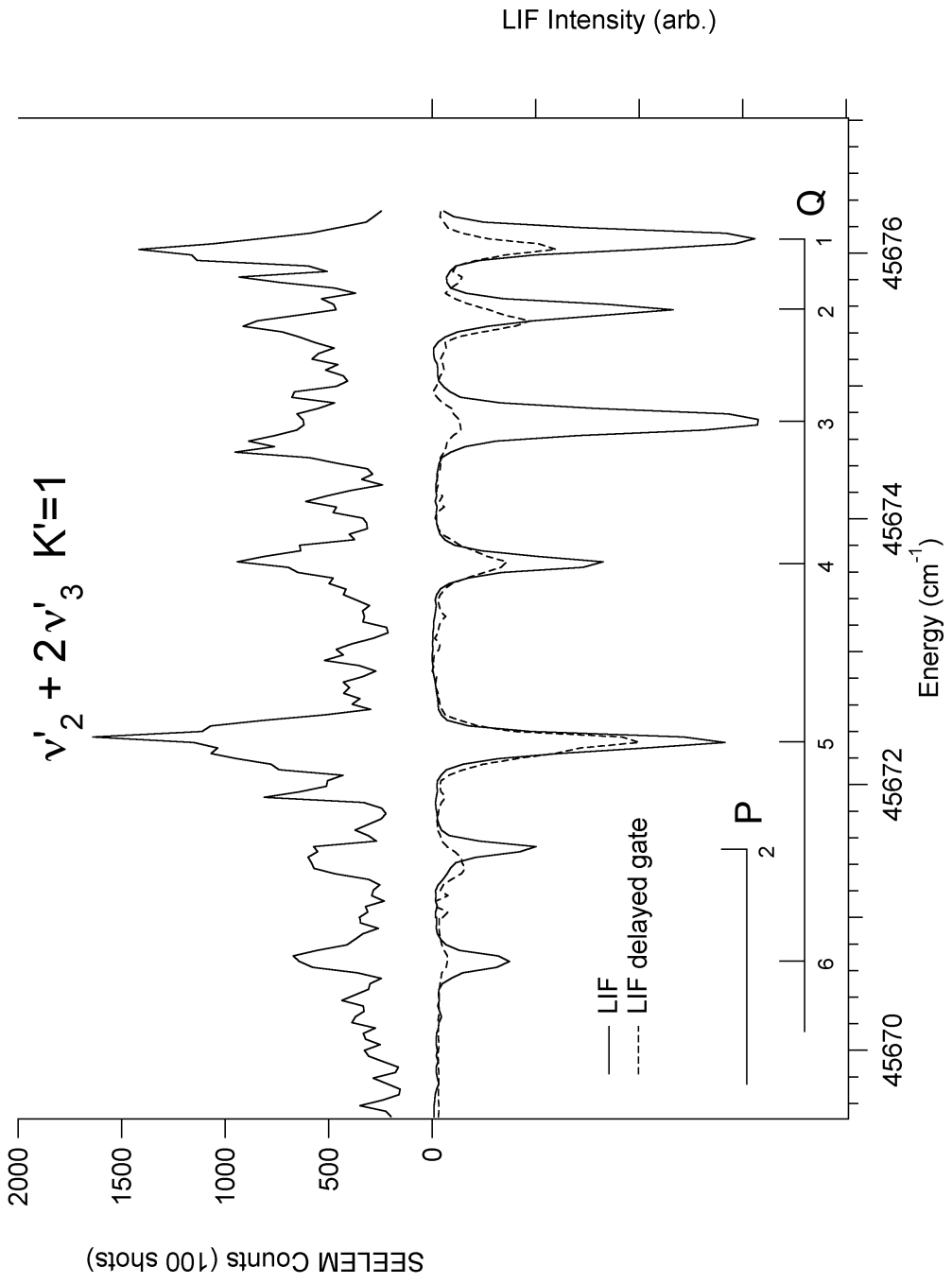

Figure 4-2: Dependence of the intensity-weighted center of gravity on delay for a series of individually resolved transitions, Q(1−5), in the LIF spectrum of the $\nu_2'+2\nu_3'$ K_a=1 sublevel. The Q(1) and Q(2) transitions arrive at peak positions identical to the those in the SEELEM spectrum by a delay of $15\tau_s$.

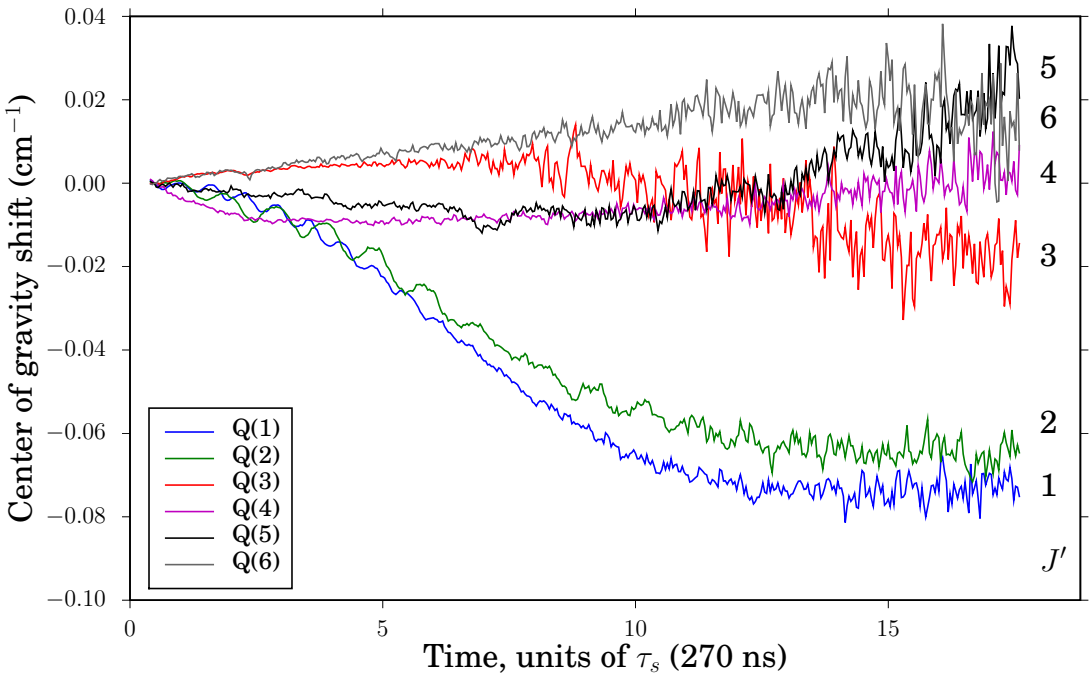

Figure 4-3: Simultaneously recorded SEELEM (upper trace) and LIF (lower trace) spectra of the $2\nu_2'+\nu_3'$ $K_a'=1$ sublevel of the $\tilde{A}^1A_u \leftarrow \tilde{X}^1\Sigma_g^+$ electronic transition. The LIF spectrum is integrated in two time regions: an early time window ($0.5\tau_s - 2\tau_s$, solid trace) and a delayed time window ($8\tau_s - 12\tau_s$, dashed trace). The Q(1) and R(0) transitions, which have the same upper state quantum number $J' = 1$ but different parities, are shifted to opposite directions in the delayed fluorescence spectrum.

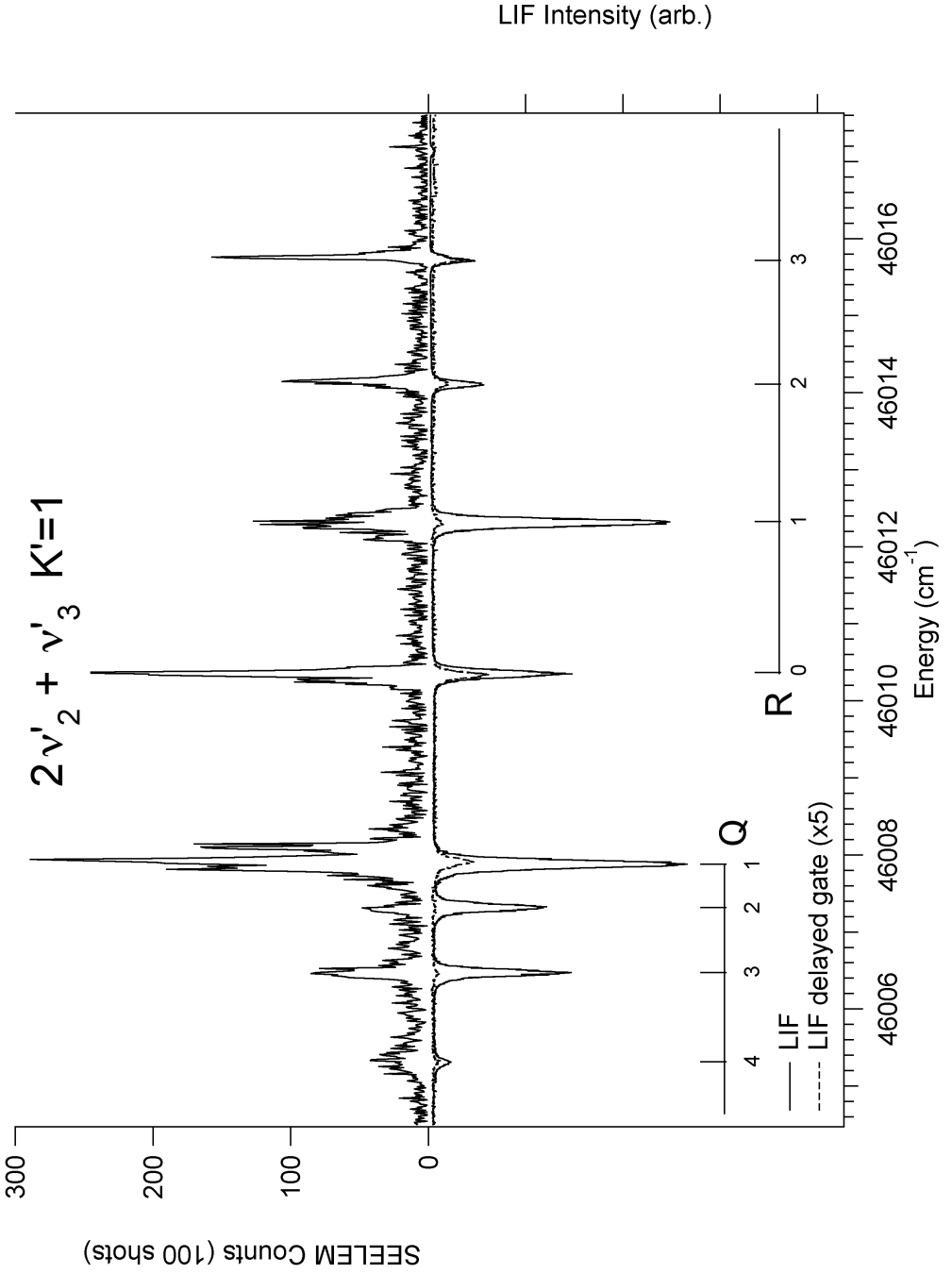

Figure 4-4: Dependence of the intensity-weighted center of gravity on delay for a series of individually resolved transitions, Q(1−4) (top), and R(0−3) (bottom), in the LIF spectrum of the $2\nu_2' + \nu_3'$ K_a=1 sublevel. The center of gravity for the Q(1) transition rapidly increases to its final value, where it matches the peak of the SEELEM distribution at 46007.87+0.03 cm^{-1}. For the R(0) transition, the center of gravity decreases at a nearly linear rate to 46010.35−0.3 cm^{-1}.

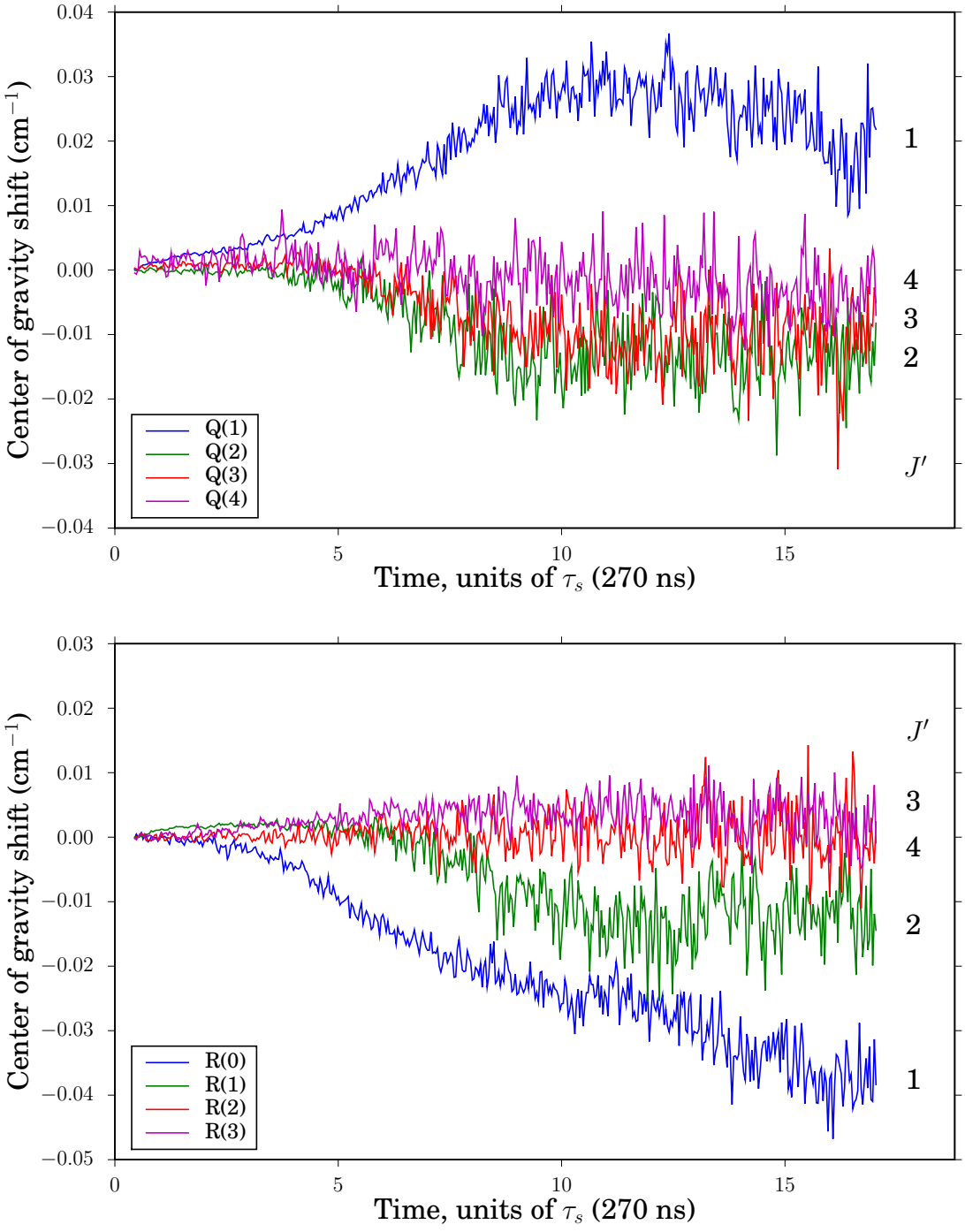

Figure 4-5: [NOT TO BE INCLUDED IN FINAL CHAPTER] Simultaneously recorded SEELEM (upper trace) and LIF (lower trace) spectra of the $2\nu_2' + \nu_3'$ K_a=1 sublevel of the $\tilde{A}^1A_u \leftarrow \tilde{X}^1\Sigma_g^+$ electronic transition, recorded at approximately 4× smaller energy intervals. The LIF spectrum is integrated in two time regions: an early time window (UNSPECIFIED, solid trace) and a delayed time window (UNSPECIFIED, dashed trace). The peak of the Q(1) transition is blueshifted in the delayed fluorescence spectrum, in contrast to the Q(2) and Q(3) transitions, which show essentially no shift.

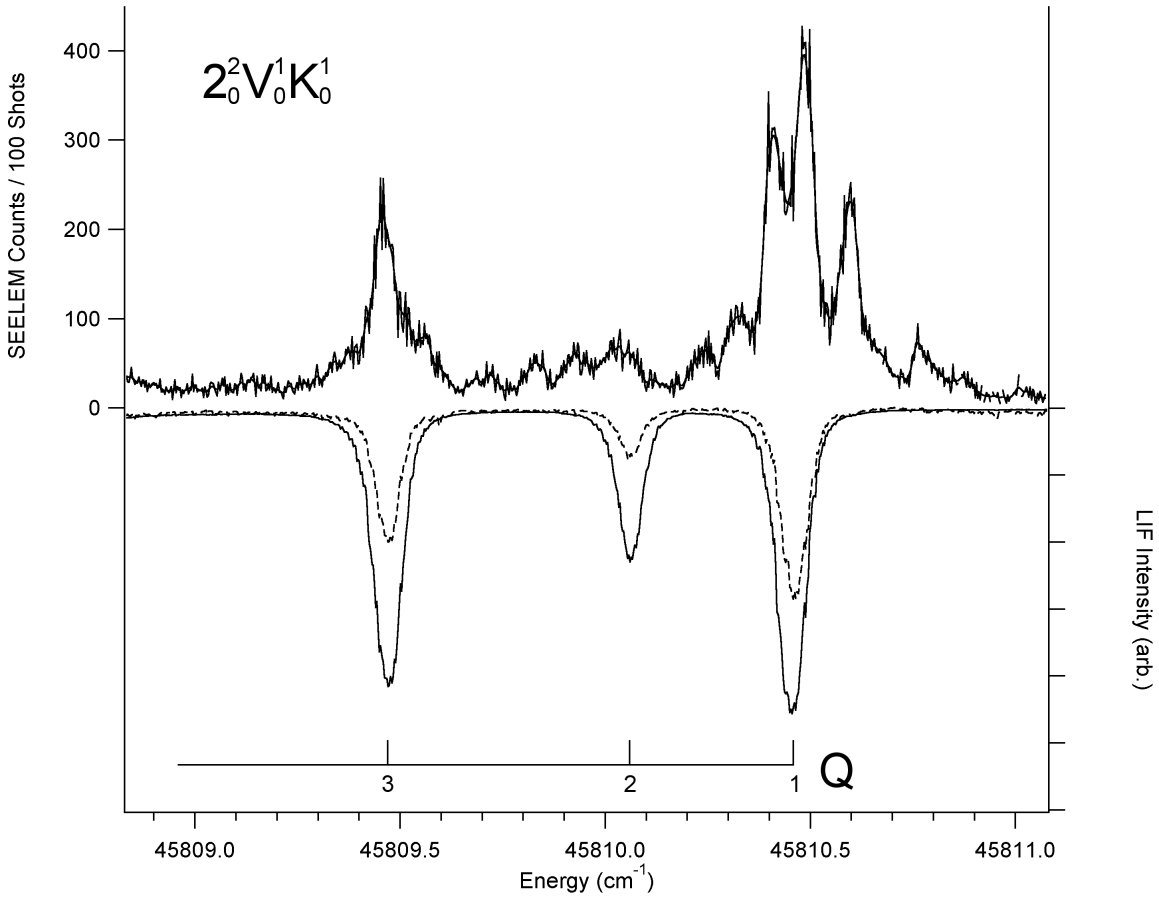

Figure 4-6: [NOT TO BE INCLUDED IN FINAL CHAPTER] Simultaneously recorded SEELEM (upper trace) and LIF (lower trace) spectra of the $2\nu_2' + \nu_3'$ K_a=1 sublevel of the $\tilde{A}^1A_u \leftarrow \tilde{X}^1\Sigma_g^+$ electronic transition, recorded at approximately 4× smaller energy intervals. The LIF spectrum is integrated in two time regions: an early time window (UNSPECIFIED, solid trace) and a delayed time window (UNSPECIFIED, dashed trace). The peak of the Q(1) transition is blueshifted in the delayed fluorescence spectrum, in contrast to the R(0) transition, which is redshifted.

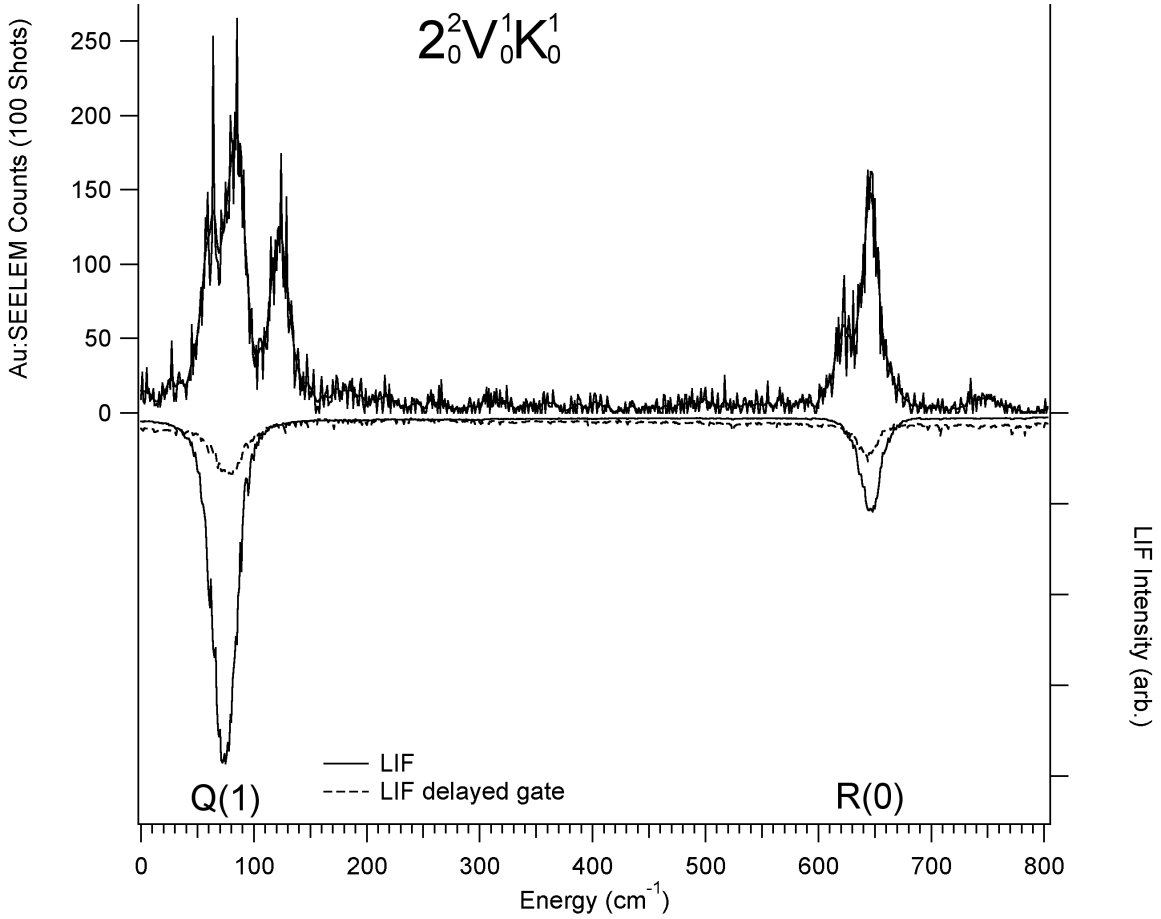

Figure 4-7: Simultaneously recorded SEELEM (upper trace) and LIF (lower trace) spectra of the $3\nu_3'$ $K_a'=2$ sublevel of the $\tilde{A}^1A_u \leftarrow \tilde{X}^1\Sigma_g^+$ electronic transition. The LIF spectrum is integrated in two time regions: an early time window ($0.5\tau_s - 2\tau_s$, solid trace) and a delayed time window ($10\tau_s - 18\tau_s$, dashed trace). The individual transitions are each split at least two strongly mixed components. Although the energy splitting between the components is on the order of the experimental resolution, they are discernable via changes in the fluorescence lineshape resulting from their differing relative intenities in the early and delayed fluorescence spectra. One splitting in the R(4) transition is just resolved in this spectrum. **TODO:** Determine the assignment for the set of overlapping transitions.

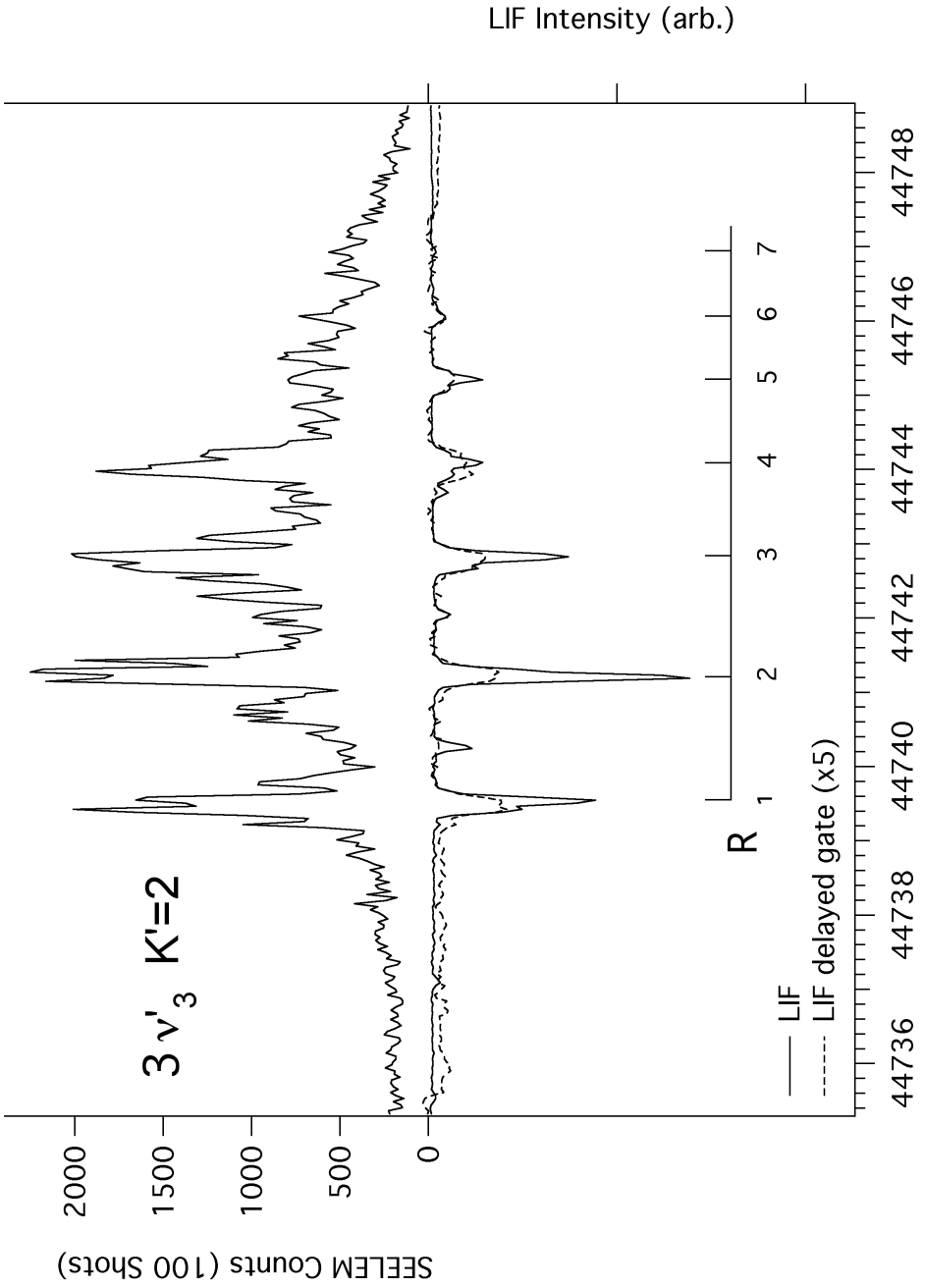

Figure 4-8: Dependence of the intensity-weighted center of gravity on delay for a series of individually resolved transitions, R(1−7), in the LIF spectrum of the $3\nu_3'$ $K_a' = 2$ sublevel. The individual transitions have an overall bias to lower energies at long delay times, indicating an interaction with a T_3 doorway level at lower energy.

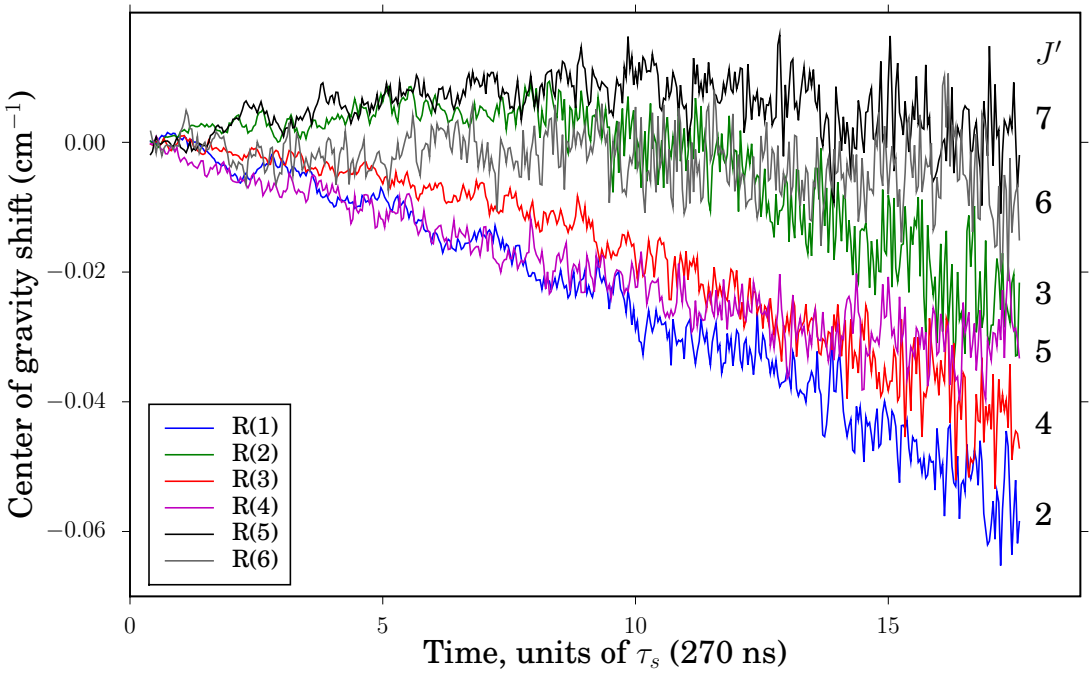

Chapter 4

SEELEM/LIF spectroscopy of acetylene: Spectral signatures of energetically distant doorway levels

4.1 $\nu_2' + 2\nu_3'$

4.2 $2\nu_2' + \nu_3'$

4.3 $3\nu_3'\ K_a' = 2$

4.4 $2\nu_3' + 2\nu_4'$

4.5 Band integrated center-of-gravity

Figure 4-9: Simultaneously recorded SEELEM (upper trace) and LIF (lower trace) spectra of the $2\nu_3' + 2\nu_4'$ $K_a' = 1$ sublevel of the $\tilde{A}^1A_u \leftarrow \tilde{X}^1\Sigma_g^+$ electronic transition. The LIF spectrum is integrated in two time regions: an early time window ($0.5\tau_s - 2\tau_s$, solid trace) and a delayed time window ($10\tau_s - 18\tau_s$, dashed trace). The peak positions are blueshifted in the delayed fluorescence spectrum for all transitions, with the exception of Q(2). Perturbations from a level of slightly lower energy are apparent in the delayed fluorescence spectrum of the Q(2) and R(1) transitions.

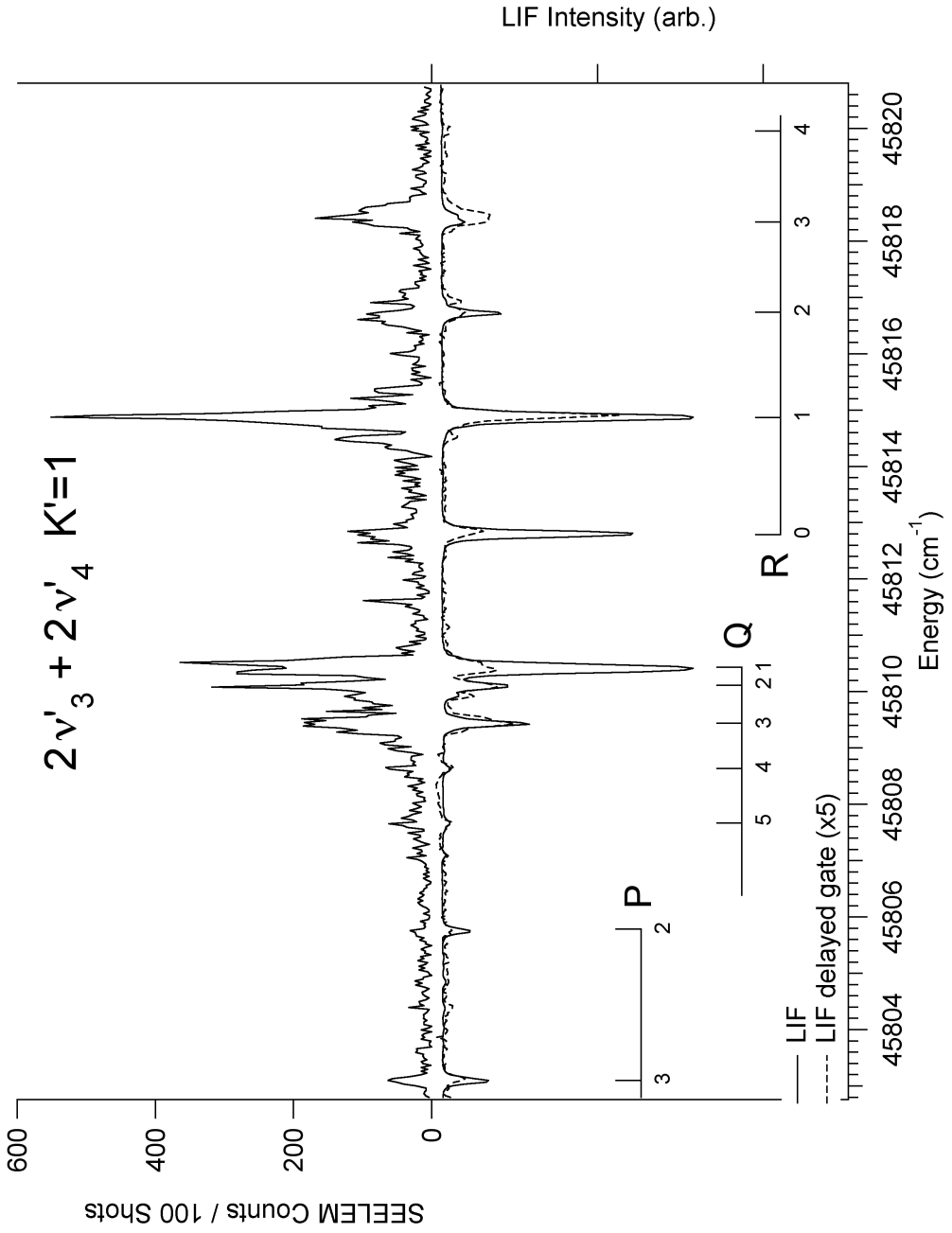

Figure 4-10: Dependence of the intensity-weighted center of gravity on delay for a series of individually resolved transitions, Q(1−3) (top), and R(0−3) (bottom), in the LIF spectrum of the $2\nu_3' + 2\nu_4'$ $K_a' = 1$ sublevel. Perturbations in the Q(2) and R(1) transitions cause the center of gravity to deviate from that of the other transitions as the delay time is increased.

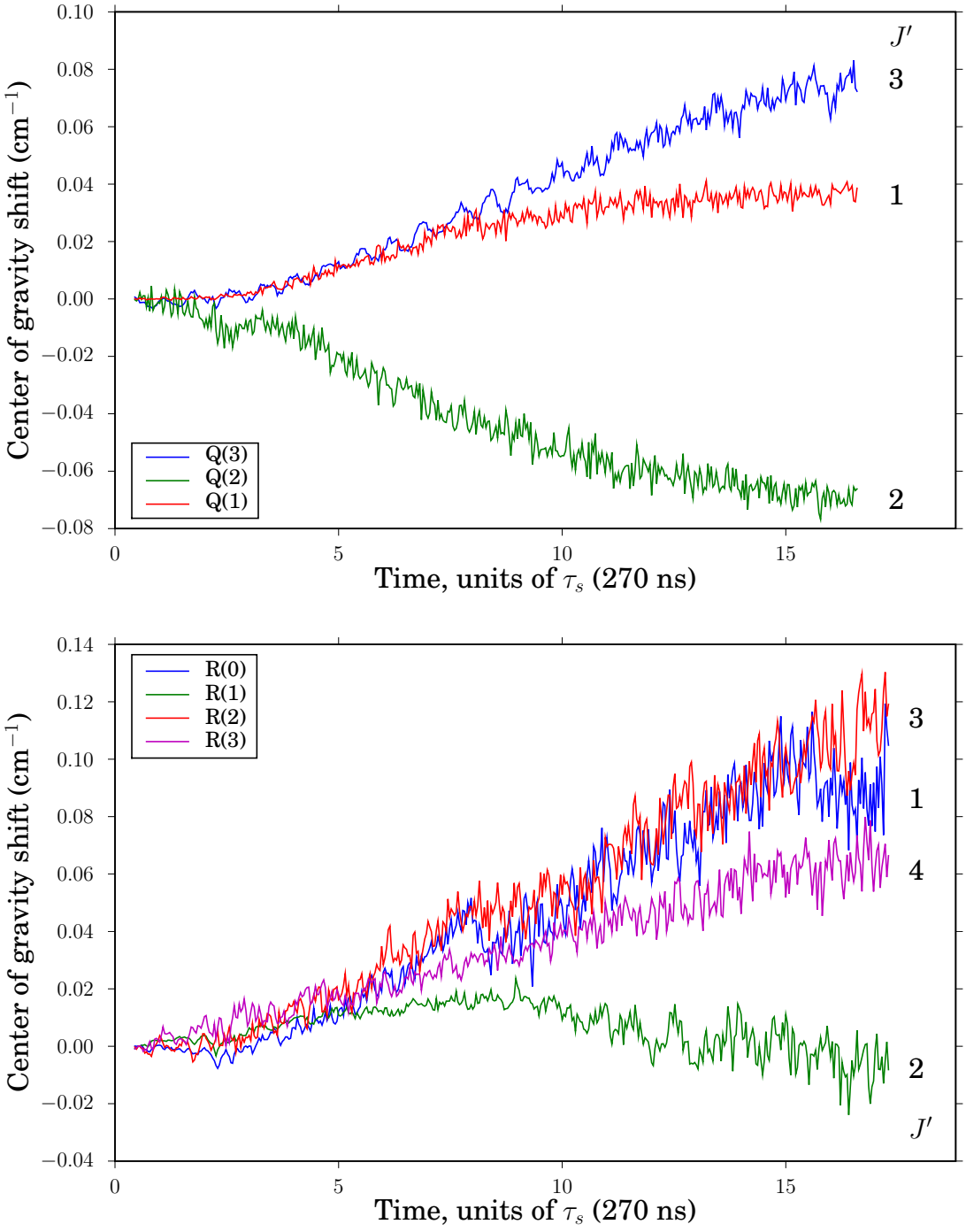

Table 4.2: Band-integrated center of gravity measurements from simultaneously recorded SEELEM/LIF spectra of $\tilde{A}\ ^1A_u$ acetylene. The SEELEM−LIF center of gravity is offset to lower energy for Q-branch measurements and offset to higher energy for R-branch measurements, indicating an overall increase in relative SEELEM:LIF intensity with J'. Such J'-dependent behavior is predicted in the presence of energetically distant T_3 doorway levels.

Q-branch measurements

Level	Integration region	Center of gravity		Offset
		LIF	SEELEM	SEELEM−LIF
$\nu_2' + 2\nu_3'$	45671.75−76.30	45674.60	45674.09	−0.51
$2\nu_2' + \nu_3'$	46004.50−08.50	46007.29	46007.23	−0.06
$2\nu_3' + 2\nu_4'$	45807.30−11.00	45810.09	45809.72	−0.37

R-branch measurements

Level	Integration region	Center of gravity		Offset
		LIF	SEELEM	SEELEM−LIF
$2\nu_2' + \nu_3'$	46009.50−16.50	46012.11	46012.49	+0.38
$3\nu_3'\ \ K'=2$	44738.50−47.50	44741.79	44742.67	+0.88
$2\nu_3' + 2\nu_4'$	45812.00−20.50	45814.67	45815.57	+0.89